Journal of Organometallic Chemistry 901 (2019) 120934

Contents lists available at ScienceDirect

Journal of Organometallic Chemistry

journal homepage: www.elsevier.com/locate/jorganchem

Heterobimetallic Ru(μ-dppm)Fe and homobimetallic Ru(μ-dppm)Ru complexes as potential anti-cancer agents

Brian Herry [a], Lucinda K. Batchelor [e], Basile Roufosse [a], Dario Romano [b, c], Judith Baumgartner [d], Marina Borzova [a], Tim Reifenstahl [a], Thomas Collins [a], Amal Benamrane [a], Jordana Weggelaar [a], Marie C. Correia [a], Paul J. Dyson [e], Burgert Blom [a, *]

[a] Maastricht Science Programme, Faculty of Science and Engineering, Maastricht University, Kapoenstraat 2, PO Box 616, 6200, MD, Maastricht, the Netherlands
[b] Department of Biobased Materials, Faculty of Science and Engineering, Maastricht University, Brightlands Chemelot Campus, Urmonderbaan 22, Geleen, 6167, RD, the Netherlands
[c] Aachen-Maastricht Institute for Biobased Materials, Brightlands Chemelot Campus, Urmonderbaan 22, Geleen, 6167, RD, the Netherlands
[d] Institut für Anorganische Chemie, Technische Universität Graz, Stremayrgasse 9, A-8010, Graz, Austria
[e] Institut des Sciences et Ingénierie Chimiques, Ecole Polytechnique Fédérale de Lausanne (EPFL), CH1015, Lausanne, Switzerland

ARTICLE INFO

Article history:
Received 22 August 2019
Received in revised form
9 September 2019
Accepted 10 September 2019
Available online 13 September 2019

Keywords:
Bioorganometallic chemistry
Heterobimetallic complexes
Homobimetallic complexes
Metal-based drugs
Cytotoxicity studies

ABSTRACT

Two heterobimetallic μ-dppm bridged Fe,Ru complexes, [(η^6-Arene)$RuCl_2$(μ-dppm)Fe(CO)I(η^5-C_5H_5)] (Ar = C_6H_6 (**1**) and *p*-cymene (**2**), dppm = 1,1-bis(diphenylphosphino)methane) were obtained in a facile reaction between [Fe(η^5-C_5H_5)I(CO)(κ^1-dppm)] (**5**) and the corresponding [(η^6-Arene)$RuCl_2$]$_2$ complexes by dimer cleavage, mediated by the pendant -PPh_2 in **5**. The homodinuclear Ru,Ru complex, [(η^6-C_6H_6)$RuCl_2$(μ-dppm)$RuCl_2$(η^6-C_6H_6)] (**3**), was also isolated in a straightforward fashion upon reaction of [(η^6-C_6H_6)$RuCl_2$(κ^1-dppm)] (**4**) with [(η^6-C_6H_6)$RuCl_2$]$_2$. All complexes were fully characterized by multinuclear (^{1}H, ^{13}C{^{1}H}, ^{31}P{^{1}H}) NMR, UV−Vis, IR spectroscopy and HRMS (ESI), and additionally complex **3** was characterized by single crystal X-ray diffraction. Density functional theory (DFT) calculations (Level of theory B3LYP, basis set for H, C, P, O, N and Cl is 6-31 + G(d,p) and for Ru,Fe DGDZVP) of **1**, **2** and **3** are also reported. Complexes **1** and **2** feature HOMOs and LUMOs delocalized over the iron-centered terminus of the bimetallic complexes. The cytotoxicity of **1**−**5** were evaluated on A2780 and A2780cisR (Human ovarian carcinoma) cell lines and the HEK293 (Human embryonic kidney) cell line. The complexes containing iron are more cytotoxic than cisplatin in the A2780 cells and significantly more active in the A2780cisR cell line and exhibit some selectivity towards the cancer cells. The dinuclear Ru,Ru complex **3** and the mononuclear complex **4** exhibit moderate activity on A2780 and A2780cisR cells also with some cancer cell selectivity. This study hence reveals the potential of Fe,Ru complexes as potent cytotoxic agents.

1. Introduction

Chemotherapies based on the metal containing compounds is one of the most widely used ways to treat cancer and platinum-based drugs are extensively used in this regard. Historically, the most prominent of these platinum drugs is cisplatin, [1] which binds to the purine base pairs of DNA, causing DNA damage and subsequently inducing apoptosis [2]. Disadvantages of cisplatin include intrinsic and acquired resistance along with toxicity leading to severe side-effects [3]. Other platinum-containing anticancer drugs such as carboplatin, oxaliplatin, nedaplatin and heptaplatin (Chart 1) have been developed that, to varying extents, overcome these disadvantages. Carboplatin and cisplatin remain extensively used drugs to treat cancer due to their extensive spectrum of activity. Oxaliplatin and nedaplatin are also approved for clinical treatment of certain cancers and heptaplatin is undergoing clinical trials [4].

* Corresponding author.
E-mail address: burgert.blom@maastrichtuniversity.nl (B. Blom).

https://doi.org/10.1016/j.jorganchem.2019.120934
0022-328X/

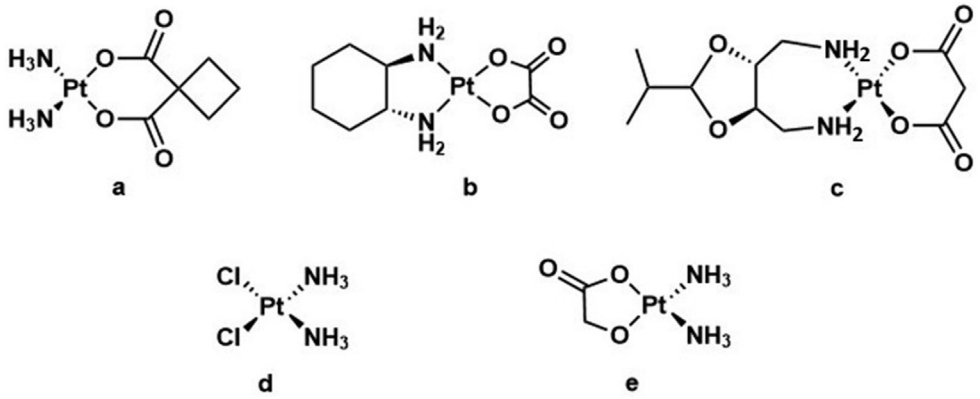

Chart 1. Structures of several platins: a. Carboplatin, b. Oxaliplatin, c. Heptaplatin, d. Cisplatin, e. Nedaplatin.

Substituting platinum by other transition metals is an alternative approach to overcome the limitations of platinum-based drugs [5]. Ruthenium complexes show substantial promise as antineoplastic agents and can potentially reduce severe side effects due to their higher selectivity towards cancer cells [6]. Ruthenium complexes have the potential to bind to a wide variety of biomolecules including DNA and histone proteins [7]. Studies also suggest that ruthenium complexes (in particular Ru(III) have the propensity to bind (or associate) to transferrin), and consequently might be a mechanism by which Ru complexes gain access to cells [8]. This notion punctuates past and even recent literature, [9] but has also been questioned [10].

A classic example of a promising Ru-based anticancer agent is RAPTA-C (Chart 2) [11]. RAPTA-C, when combined with other drugs, shows a reduction in tumour growth of up to 80% without serious side effects [12]. Other notable examples of promising ruthenium-based agents are NAMI-A and KP1019 [13,14].

Another strategy is to incorporate two metal centres, exploiting their distinct biological and pharmacological features into one well-defined molecular complex. The interactions of two distinct metal centres may result in a synergic influence on cytotoxicity compared to their monometallic counterparts [15]. In this regard, systems bearing Ru and Au centres bridged by a dppm ligand (Chart 3), have been reported and the bimetallic complexes are more active than their monometallic precursors [5i].

Inspired by these findings we decided to target heterobimetallic Fe,Ru complexes and elucidate their *in vitro* cytotoxicity. Since some piano-stool Cp (η^5-C_5H_5) iron complexes are cytotoxic in their own right, [16] we hypothesized that a possible synergistic effect might also be found on combination with RAPTA-like complexes, as with the earlier reported Ru,Au complexes (see above). Surprisingly, heterobimetallic μ-phosphane Fe,Ru complexes are somewhat rare [17] and, to the best of our knowledge, their anti-cancer properties have not been investigated. Herein, we report on the facile entry to two related Fe,Ru complexes, [(η^6-Arene)$RuCl_2$(μ-dppm)Fe(CO)I(η^5-C_5H_5)] (Arene = C_6H_6 (**1**) or *p*-cymene (**2**), dppm = 1,1-bis(diphenylphosphino)methane and compare their cytotoxicity to a related homodinuclear Ru,Ru complex [(η^6-C_6H_6)$RuCl_2$(μ-dppm)$RuCl_2$(η^6-C_6H_6)] (**3**) as well as the mononuclear complexes [(η^6-C_6H_6)$RuCl_2$(κ^1-dppm)] (**4**), [Fe(η^5-C_5H_5)I(CO)(κ^1-dppm)] (**5**).

2. Results and discussion

2.1. Synthesis and characterisation

Complexes **1** and **2** were prepared by reacting [Fe(η^5-C_5H_5)I(CO)(κ^1-dppm)] (**5**), reported in 1972 by Haines and du Preez [18] with [(η^6-C_6H_6)$RuCl_2$]$_2$ and [(η^6-*p*-cymene)$RuCl_2$]$_2$, respectively, in a 2:1 ratio in dichloromethane. The reactions were monitored by TLC tracing the consumption of the green complex **5** (typically within *ca.* 1 h) and the complexes were isolated as dark brown solids in good to excellent yield (Scheme 1).

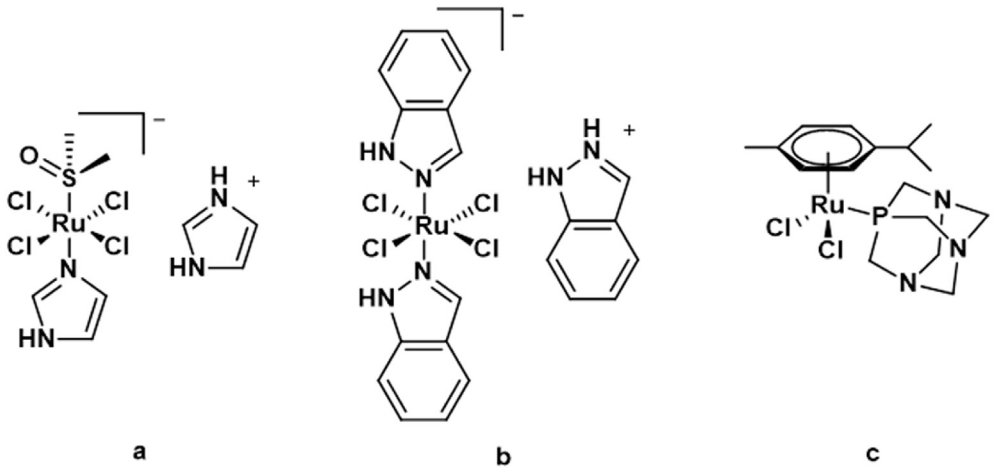

Chart 2. Cytotoxic ruthenium based complexes: a. NAMI-A, b. KP1019, c. RAPTA-C.

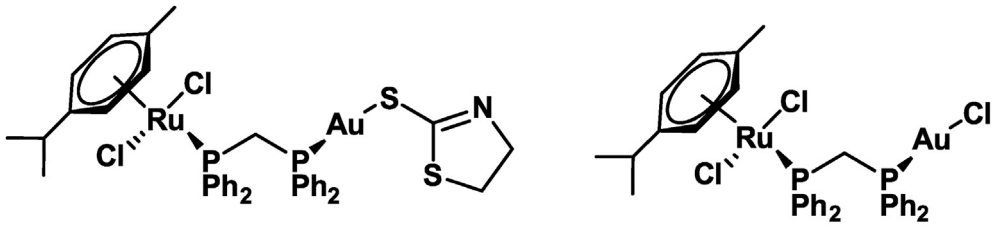

Chart 3. Heterobimetallic Ru,Au complexes showing promising anti-cancer activity [5i].

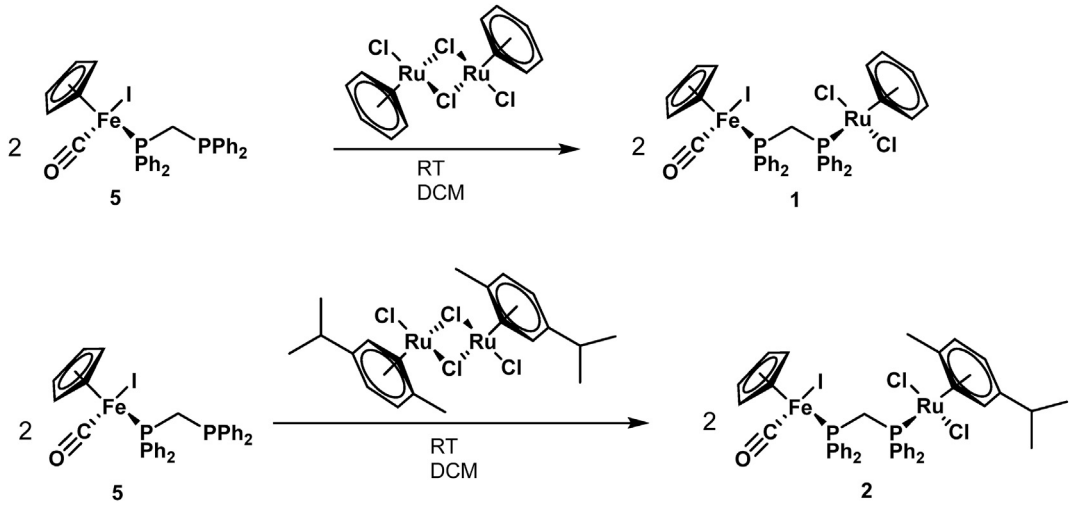

Scheme 1. Synthesis of heterobimetallic Fe,Ru complexes **1** and **2**.

Complexes **1** and **2** exhibit two sets of doublet resonance signals in their respective $^{31}P\{^{1}H\}$ NMR spectra indicative of coordination to two distinct metal centres with the high field shifted resonance corresponding to Ru—P coordination, and the lower field shifted doublet resonance signal corresponding to Fe—P coordination (**1:** 63.8 (d, $^{2}J_{PP} = 45.0$ Hz, Fe-PPh_2), 24.5 (d, $^{2}J_{PP} = 44.5$ Hz, Ru-PPh_2; **2:** 63.2 (d, $^{2}J_{PP} = 44.1$ Hz, Fe-PPh_2), 24.1 (d, $^{2}J_{PP} = 43.9$ Hz, Ru-PPh_2). The ^{1}H NMR spectra of **1** and **2** exhibit some line broadening for both complexes which might be due to the presence of trace amounts of paramagnetic impurities, or paramagnetic cross-over at the Fe(II) centre [19]. Nevertheless, a full assignment of their ^{1}H NMR spectra was possible for both complexes. In particular, for **1**, singlets corresponding to the metal bound η^5-C_5H_5 ($\delta = 4.04$ ppm) and η^6-C_6H_6 ($\delta = 4.70$ ppm) ligands are observed as broad singlets. In complex **2** the resonances for the η^6-p-cymene are observed as a series of complex multiplets while the η^5-C_5H_5 ligand affords a singlet ($\delta = 4.00$ ppm). In both complexes the methylene bridge between the two P atoms of the dppm ligand exhibit two distinct sets of broad multiplets, corresponding to diastereotopic CH^AH^B atoms. The IR spectra of **1** and **2** contain a characteristic ν(CO) stretching vibration at 1937 cm^{-1} compared to the iron precursor **5** at 1944 cm^{-1}. In both complexes a weak signal in the electron impact mass spectrum (EI-MS) could be detected corresponding to the mass of the complex at the corresponding *m/z*, and the $[M+Na]^+$ ion was detected in the high resolution electrospray ionisation mass spectrum (ESI-MS) for both complexes further confirming their constitution.

The synthesis of the homodinculear Ru,Ru dimer **3** was achieved via reaction of [$RuCl_2(\eta^6$-$C_6H_6)(\kappa^1$-dppm)] (**4**) [20] with [$(\eta^6$-$C_6H_6)RuCl_2]_2$ in a 2:1 ratio to selectively afford **3** in high yield (Scheme 2). The *p*-cymene analogue of **3** i.e. [$(RuCl_2(\eta^6$-*p*-cymene$))_2(\mu$-dppm)] (**3-cym**) has been reported previously [21].

We attempted to prepare the asymmetric complex [$RuCl_2(\eta^6$-$C_6H_6)(\mu$-dppm)$RuCl_2(\eta^6$-*p*-cymene)] (i.e. with different arenes on each metal centre) by reacting **4** with the dimer [$(\eta^6$-*p*-cymene)$RuCl_2]_2$ (2:1 ratio), or the other way around, i.e. reacting [$RuCl_2(\eta^6$-*p*-cymene)$(\kappa^1$-dppm)] **(4-cym)** [22] with [$(\eta^6$-$C_6H_6)RuCl_2]_2$. In both cases, the desired asymmetric complex was not obtained, instead 1:1 mixtures of the symmetrical dimer complexes **3** and **3-cym** were observed, on the basis of ^{31}P and ^{1}H NMR spectroscopy and ESI-MS. This result can possibly be understood by considering dppm decomplexation equilibria from **4** (or **4-cym**) affording free

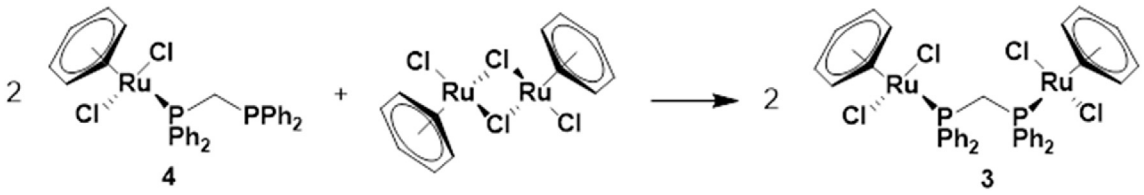

Scheme 2. Synthesis of the symmetrical homobimetallic Ru,Ru complex **3**.

dppm, which then reacts with the dimer $[(\eta^6\text{-Arene})RuCl_2]_2$ rapidly affording the distribution of products observed. The desired asymmetric complexes might form *in situ* but subsequently rearrange to their symmetrical counterparts [23].

Complex **3** features a singlet in the $^{31}P\{^1H\}$ NMR spectrum at $\delta = 22.6$ ppm. The ^1H NMR spectrum (in $CDCl_3$) shows the characteristic singlet resonance signal for the η^6 coordinated benzene at $\delta = 5.31$ ppm and the methylene protons in the μ-dppm bridge as a triplet (due to P,H coupling) centered at $\delta = 4.7$ ppm. The structure of **3** was corroborated by HRMS which showed the adduct $[M+Na]^+$: $m/z = 906.8844$ (expt.) Found: 906.8842. We obtained crystals, suitable for single crystal X-ray diffraction analysis of **3** by slow evaporation of a concentrated dichloromethane solution of the complex. The solid-state structure of **3** is show in Fig. 1. At both Ru centres in the benzene rings are coordinated in an η^6-fashion since the Ru–C bonds lengths are comparable to each other within narrow limits (in Ru1 this ranges from 2.179(5) Å – 2.232(5) Å). The metal centres in both cases may be described as having distorted octahedral geometries, with the benzene rings occupying three coordination sites, and the other sites being occupied by two chlorido ligands and the P atom of the μ-dppm. The bond angles around the Ru centres are close to 90° in accordance with this geometry. Note that viewing the structure down the Ru–Ru axis reveals a staggered configuration of the two metal bound arene ring systems. The phenyl rings in the μ-dppm seem to exhibit quasi-parallel planes of phosphorous bound phenyl rings, possibly due to π-π stacking.

2.2. Density functional theory calculations

In order to probe the electronic structure of **1**, **2** and **3**, we undertook density functional theory (DFT) investigations (Level of theory B3LYP, basis set for H, C, P, O, N and Cl is 6-31 + G(d,p) and for Ru,Fe DGDZVP). We decided to focus our attention on the location of the frontier orbitals to gain insights into the reactivity of the complexes *in vitro*. Since we were unable to obtain an X-ray structure of complex **1** and **2**, we also relied on the optimized structures for structural information (see Fig. 2).

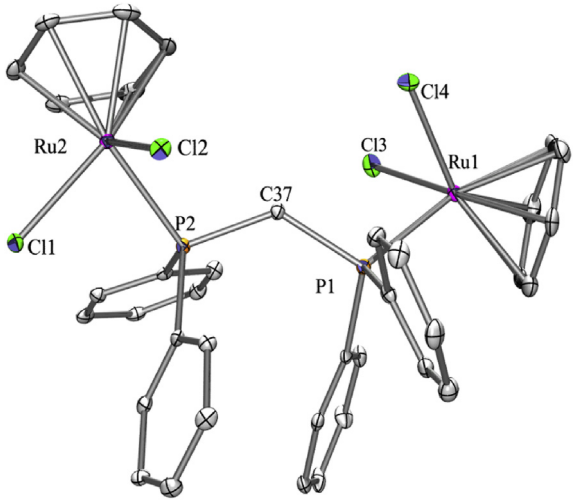

Fig. 1. ORTEP representation of the solid-state structure of **3** determined by X-ray diffraction. Thermal ellipsoids are set at the 30% probability level. All H atoms omitted for clarity. Selected bond lengths [Å]: Ru(1)–C(5) 2.179(5), Ru(1)–C(3) 2.182(5), Ru(1)–C(6) 2.188(5), Ru(1)–C(1) 2.196(5), Ru(1)–C(2) 2.196(5), Ru(1)–C(4) 2.232(5), Ru(1)–P(1) 2.3543(12), Ru(1)–Cl(4) 2.4024(12), Ru(1)–Cl(3) 2.4088(12), Ru(2)–C(23) 2.154(4), Ru(2)–C(21) 2.174(5), Ru(2)–C(19) 2.180(5), Ru(2)–C(24) 2.190(5), Ru(2)–C(22) 2.209(5), Ru(2)–C(20) 2.253(5), Ru(2)–P(2) 2.3442(12), Ru(2)–Cl(2) 2.4116(11), Ru(2)–Cl(1) 2.4132(11). Selected bond angles [°]: P(1)-Ru(1)-Cl(4) 87.17(4), P(1)-Ru(1)-Cl(3) 87.49(4), Cl(4)-Ru(1)-Cl(3) 86.50(5), P(2)-Ru(2)-Cl(2) 86.98(4), P(2)-Ru(2)-Cl(1) 84.62(4), Cl(2)-Ru(2)-Cl(1) 90.43(4).

Both complexes exhibit a *syn* configuration of the Fe,Ru moieties, akin to that of Ru,Ru dimer **3** (see above). Indeed, the optimized geometries of **1** and **2** are strikingly similar to those obtained by X-Ray diffraction analysis of **3**.

The HOMOs and LUMOs of **1** and **2** (Fig. 3) are similar and both are located on the same group of atoms, indicating that change from benzene to *p*-cymene has little effect. In particular, the HOMOs are mainly located on the group of Fe–CO axis and extend over the iodine atoms. The LUMOs are localised on the iron atom and involves mainly one phenyl group on the coordinated phosphine ligand, with some delocalization over the Cp ring. For both **1** and **2**, the energy values for the HOMO and LUMO are essentially the same. The locality of both frontier orbitals on the iron moiety indicates that reactivity of **1** and **2** would be initiated there, rather than at the ruthenium center. The calculated HOMO-LUMO gap for complex **1** is 3.88 eV which corresponds to a calculated λ_{max} absorption value of 319 nm. This compared fairly well with the experimental value of 365 nm. Similarly, complex **2** features a HOMO-LUMO separation of 3.9 eV, corresponding to a calculated λ_{max} absorption value of 318 nm which also compares well with the experimental value of 357 nm. The differences arise from the fact that the calculations were carried out in the absence of solvation.

For comparison, the location of the frontier orbitals (HOMO and LUMO) for the homobimetallic complex **3** is shown in Fig. 4.

The shapes of the frontier orbitals for **3** are similar to **1** and **2**. However, the HOMO and the LUMO involve *both* ruthenium atoms in the complexes, in contrast **1** and **2**. Notably, the optimized structure obtained by DFT of **3** is in excellent agreement with the experimentally determined X-ray structure and the metrical parameters are comparable.

2.3. In vitro cytotoxicity investigations

The cytotoxicity of complexes **1**–**5** was evaluated on Human Ovarian Carcinoma cell lines (A2780 and A2780cisR, the latter with acquired resistance to cisplatin) and non-tumorigenic Human Embryonic Kidney Cells (HEK293) together with cisplatin and RAPTA-C as a positive (0–100 μM) and negative (200 μM) controls, respectively (see Table 1). Remarkably, complex **5** reported in 1972, has escaped cytotoxic investigations and was included in the study for comparison.

The cytotoxicity studies reveals that the iron containing complexes (**1**, **2** and **5**) are considerably more cytotoxic than the mononuclear ruthenium complex (**4**) or its dinuclear counterpart (**3**). The iron containing complexes exhibit similar activities on both the A2780 and A2780cisR cell lines with **2** being more cytotoxic than cisplatin on the A2780 cell line. The iron containing complexes (**1**, **2** and **5**) overcome resistance in the A2780cisR cell line, i.e. they exhibit similar cytotoxicities in both the A2780 and A2780cisR cell lines, in the range 1.2–2.2 μM, with **2** and **5** also displaying a modest degree of cancer cell selectivity in that about twice the concentration is required to afford an IC_{50} value in the HEK293 cells. Interestingly, the homodinuclear complex **3** is less cytotoxic than its mononuclear counterpart **4** in the A2780 and HEK293 cell lines. The marked decrease in cytotoxicity of complex **3** vs **4** is possibly due to retarded uptake in the cell, and can potentially be explained by the size of complex **3** which might encounter difficulties crossing the cell membrane. It is indeed instructive to compare this result with the *enhanced* cytotoxicity of the heterobimetallic dinuclear complex **2** where the trend goes in the opposite direction and having iron instead of ruthenium present in the complex boosts cytotoxicity. Overall this shows that having iron vs ruthenium present in the dinculear complexes enhances cytotoxicity.

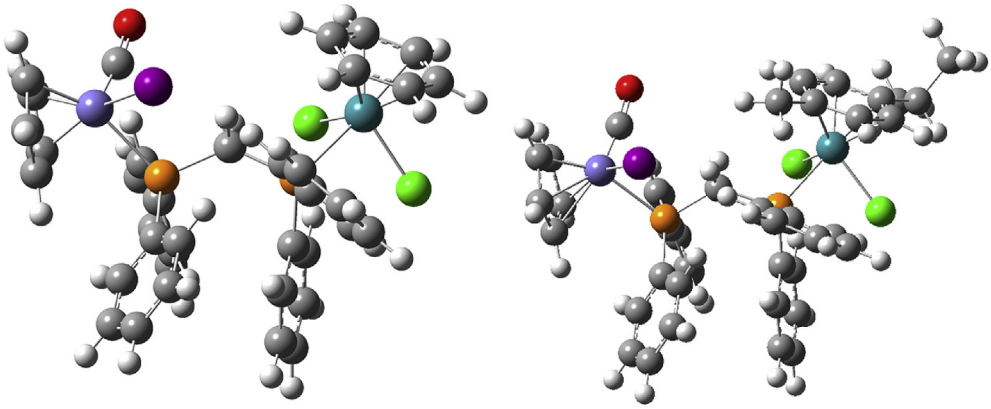

Fig. 2. Optimized structures of **1** (left) and **2** (right). (Blue = Fe, Purple = I, Orange = P, Cyan = Ru, Red = O, Green = Cl, Grey = C, White = H).

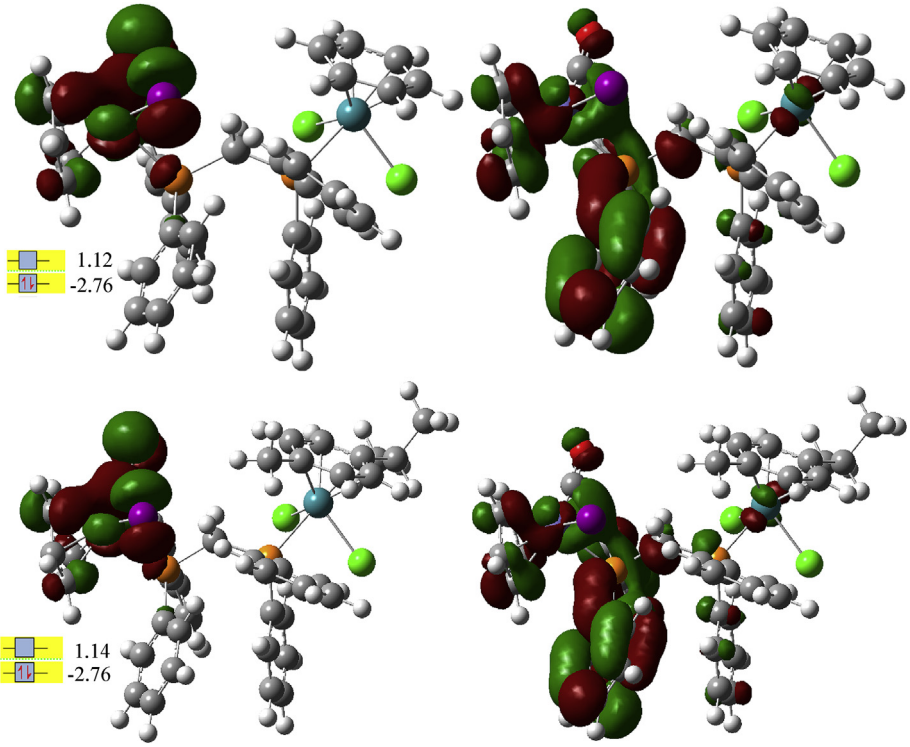

Fig. 3. Boundary surface representations of HOMO (left) and LUMO (right) for complexes **1** (top) and **2** (bottom) and relative energies (HOMO bottom and LUMO top in eV). (Purple = I, Orange = P, Cyan = Ru, Red = O, Green = Cl, Grey = C, White = H).

3. Conclusions

Facile synthetic entry to heterobimetallic Fe,Ru complexes (**1** and **2**) and a homodinuclear Ru,Ru complex (**3**) have been reported. DFT calculations reveal, as expected, localization of the HOMO and LUMOs on the iron centered part of the heterobimetallic complexes. The *in vitro* cytotoxicity of the bimetallic complexes towards tumorigenic A2780 and A2780cisR cells has also been reported compared to non-tumorigenic HEK293 cells and, notably, the heterobimetallic Fe,Ru complexes are highly cytotoxicity, overcoming cisplatin resistance with some selectivity towards cancer cells. These results indicate, for the first time, the potential of heterobimetallic Fe,Ru phosphane bridged complexes as potential anticancer agents. The mechanism of action *in vitro* requires further investigation. Further work is underway in our laboratory to explore other heterobimetallic systems and similar cooperative effects, and will be reported in subsequent communications.

4. Experimental

4.1. General considerations

All reactions were conducted under a nitrogen atmosphere at room temperature using standard Schlenk line and glove-box techniques unless otherwise stated. Reagents were obtained from commercial sources and used as received. Dimethylsulfoxide D6 (99,80%, D) was purchased from VWR Chemicals. Toluene (anhydrous, 99,8%), Dicarbonylcyclopentadienyliodoiron (II) (97%), 1,1-

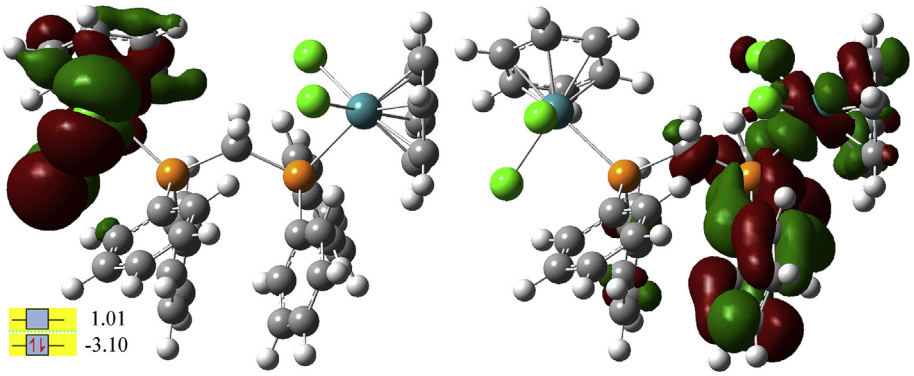

Fig. 4. Boundary surface representations of HOMO (left) and LUMO (right) for **3** and relative energies (HOMO bottom and LUMO top in eV). (Cyan = Ru, Red = O, Green = Cl, Grey = C, White = H).

Table 1
IC_{50} values (μM) of **1**–**5**, cisplatin and RAPTA-C after 72 h drug exposure. Values are represented as the mean ± SD of two or more independent experiments.

Complex	A2780			A2780cisR			HEK293		
1	2.2	±	0.1	1.5	±	0.1	2.2	±	0.1
2	1.4	±	0.1	1.2	±	0.1	2.6	±	1
3	30	±	2	16	±	1	34	±	2
4	16	±	1.2	13.8	±	0.8	18	±	1.6
5	2.1	±	0.1	1.5	±	0.1	4.5	±	0.9
cisplatin	2.3	±	0.3	17.6	±	0.5	7.6	±	1.1
RAPTA-C	<200			<200			<200		

bis(diphenylphosphino)methane (97%), η^6-benzene-ruthenium(II) chloride dimer, (η^6-*p*-cymene)-ruthenium(II) chloride dimer and silica gel (technical grade, 60 Å pore size, 70–230 mesh, 63–200 μm) were purchased from Sigma-Aldrich. n-hexane (AR grade), toluene (HPLC), and dichloromethane (stab. Amylene) were purchased from Biosolve Chimie SARL. Neutral TLC Silica 60 F_{254} sheets were used for thin layer chromatography and the aforementioned silica gel was used for column chromatography. [$RuCl_2(\eta^6\text{-}C_6H_6)(\kappa^1$-dppm)] **(4)** and [CpFe(CO)I(κ^1-dppm)] (**5**), **3-cym** and **4-cym** were prepared according to a literature procedures (see SI). All solvents, with the exception of toluene, were dried on a short plug of alumina oxide column and were purged with Nitrogen gas. A SMP10 (Stuart equipment) was used to measure melting points. A GCMS-QP2010Ultra (Shimadzu) was used to acquire mass spectra using electron impact (EI) mass spectrometry by direct injection. The software used for data interpretation was GCMS Real Time Analysis (Admin). A 300 MHz Ultrashield™ Magnet System (Bruker) was used for NMR experiments at ambient temperature. Chemical shifts for ^{1}H and ^{13}C NMR were measured relative to tetramethylsilane (TMS). For ^{31}P NMR, the chemical shifts were measured relative to phosphoric acid (85%), using Topspin 3.5pl7 software. A MIRacle 10 (single reflection ATR accessory, Shimadzu) was used to acquire FTIR spectra (Happ-Genzel apodisation, 64 scans, resolution 2) with the software IR solution. A UV-188 spectrophotometer (Shimadzu), and quartz suprasil precision cells (type 100-QS, 10 mm light path; Hellma Analytics) were used to obtain UV–Vis spectra. High resolution Electron Ionisation Spray (ESI) mass spectra were recorded using an Orbitrap LTQ XL of Thermo Scientific mass spectrometer at the Technische Universitaet Berlin. Raw data was evaluated and processed using the X-calibur computer program. In all cases the isotope distribution pattern of the signal was checked against theory. All values reported related to the line of highest intensity in the isotope pattern.

4.2. Cytotoxicity tests

Human ovarian carcinoma (A2780 and A2780cisR) cell lines were obtained from the European Collection of Cell Cultures. The human embryonic kidney (HEK-293) cell line was obtained from ATCC (Sigma, Buchs, Switzerland). Penicillin streptomycin, RPMI 1640 GlutaMAX (where RPMI = Roswell Park Memorial Institute), and DMEM GlutaMAX media (where DMEM = Dulbecco's modified Eagle medium) were obtained from Life Technologies, and fetal bovine serum (FBS) was obtained from Sigma. The cells were cultured in RPMI 1640 GlutaMAX (A2780 and A2780cisR) and DMEM GlutaMAX (HEK-293) media containing 10% heat-inactivated FBS and 1% penicillin streptomycin at 37 °C and CO2 (5%). The A2780cisR cell line was routinely treated with cisplatin (2 μM) in the media to maintain cisplatin resistance. The cytotoxicity was determined using the 3-(4,5-dimethyl 2-thiazolyl)-2,5-diphenyl-2H-tetrazolium bromide (MTT) assay [24]. Cells were seeded in flat-bottomed 96-well plates as a suspension in a prepared medium (100 μL aliquots and approximately 4300 cells/well) and preincubated for 24 h. Stock solutions of compounds were prepared in DMSO and were diluted in medium. The solutions were sequentially diluted to give a final DMSO concentration of 0.5% and a final compound concentration range (0–200 μM). Cisplatin and RAPTA-C were tested as a positive (0–100 μM) and negative (200 μM) controls respectively. The compounds were added to the preincubated 96-well plates in 100 μL aliquots, and the plates were incubated for a further 72 h. MTT (20 μL, 5 mg/mL in Dulbecco's phosphate buffered saline) was added to the cells, and the plates were incubated for a further 4 h. The culture medium was aspirated and the purple formazan crystals, formed by the mitochondrial dehydrogenase activity of vital cells, were dissolved in DMSO (100 μL/well). The absorbance of the resulting solutions, directly proportional to the number of surviving cells, was quantified at 590 nm using a SpectroMax M5e multimode microplate reader (using SoftMax Pro software, version 6.2.2). The percentage of surviving cells was calculated from the absorbance of wells corresponding to the untreated control cells. The reported IC50 values are based on the means from two independent experiments, each comprising four tests per concentration level.

4.3. X-ray structure determination

For X-ray structure analysis of complex **3** the crystals were mounted onto the tip of glass fibers, and data collection was performed with a BRUKER-AXS SMART APEX CCD diffractometer using graphite-monochromated Mo Kα radiation (0.71073 Å). The data were reduced to F^2_0 and corrected for absorption effects with SAINT

[25] and SADABS [26,27] respectively. Structures were solved by direct methods and refined by full-matrix least-squares method (SHELXL97 and SHELX2013) [28]. All non-hydrogen atoms were refined with anisotropic displacement parameters. Hydrogen atoms were placed in calculated positions to correspond to standard bond lengths and angles. All diagrams were drawn with 30% probability thermal ellipsoids and all hydrogen atoms were omitted for clarity.

4.4. Synthesis of [(η^6-C_6H_6)$RuCl_2$(μ-dppm)Fe(CO)I(η^5-C_5H_5)] (1)

0.094 g (0.14 mmol) of [CpFe(CO)(κ^1-dppm)I] and 0.037 mg (0.074 mmol) of [Ru(η^6-C_6H_6)Cl_2]$_2$ were dissolved in 26 mL of dried dichloromethane, and stirred for 1 h. The progress of the reaction was monitored by thin layer chromatography in 60:40 mixture of dichloromethane and n-hexane every 10 min. TLC showed complete consumption of starting material after 40 min of reaction. The solvent was removed *in vacuo* to isolate the solid and was washed with dried n-hexane (3 × 2 mL). After decanting the washings, the solid was dried *in vacuo* at room temperature. Air stable. 0.106 g (0.116 mmol). Dark brown solid (78.5%). Melting point 207 °C + dec. ^{1}H NMR ($CDCl_3$, 298.2 K): δ 7.64–7.52 (8H, br m, C–*H*, dppm), 7.40–7.37 (4H, br m, C–*H*, dppm), 7.16–7.06 (8H, br m, C–*H*, dppm), 5.24 (6H, s, η^6-C_6H_6), 4.32 (5H, s, η^5-C_5H_5), 3.58 (1H, br m, H^A, PCH_2P), 3.48 (1H, br m, H^B, PCH_2P). ^{13}C {^{1}H} NMR ($CDCl_3$, 298.2 K): δ 134.5–133.8 (br m, dppm), 132.5 (br s, dppm), 131.9 (br s, dppm), 131.1–129.9 (br m, dppm), 127.7 (br m, dppm), 88.6 (s, η^6-C_6H_6), 82.5 (s, η^5-C_5H_5), (PCH_2P and Fe*C*O not visible despite high concentrations and very high scan rate ca. 5 k scans). ^{31}P {^{1}H} NMR ($CDCl_3$, 298.2 K): δ 63.8 (d, $^2J_{PP}$ = 45.0 Hz, Fe-PPh_2), 24.5 (d, $^2J_{PP}$ = 44.5 Hz, Ru-PPh_2). ^{1}H NMR (C_6D_6, 298.2 K): δ 7.79 (8H, br m, C–*H*, dppm), 6.88 (12H, br m, C–*H*, dppm), 5.18 (1H, m, H^A, PCH_2P), 5.02 (1H, m, H^B, PCH_2P), 4.70 (6H, s, η^6-C_6H_6), 4.04 (5H, s, η^5-C_5H_5). ^{31}P {^{1}H} NMR (C_6D_6, 298.2 K): δ 64.0 (d, $^2J_{PP}$ = 45.0 Hz, Fe-PPh_2), 25.4 (d, $^2J_{PP}$ = 44.7 Hz, Ru-PPh_2). FTIR: 3663 (vw), 2963 (br, m), 2922 (br, m), 1937 (s, C≡O streching), 1670 (vw), 1585 (vw), 1572 (vw), 1483 (m), 1433 (s), 1315 (vw), 1260 (s), 1186 (vw), 1157 (vw), 1090 (br, vs), 1016 (br, vs), 862 (vw), 797 (vs), 731 (s), 692 (vs), 623 (w), 608 (m), 565 (br, m). UV–Vis: (nm)/dichloromethane λ_{max} = 365.0. EIMS (70 eV) *m/z* 910.50 (<0.1%, M$^+$), 384.15 (2.76%, $(Ph)_2P(CH_2)P(Ph)_2$), 400.20 (36.45%, O=$P(Ph)_2(CH_2)P(Ph)_2$), 416.20 (0.59%, O=$P(Ph)_2(CH_2)(Ph)_2P$=O), 551.15 (18.93%, [Ru(η^6-C_6H_6)Cl_2]$_2$), 678.05 (18.85%, CpFe(CO)(κ^1-dppm)I + H_2O adduct). TGA (Weight % decrease): 108.74 °C - 113.21 °C (2.372%), 187.97 °C - 188.78 °C (2.893%), 268.22 °C - 273.80 °C (6.203%), 351.10 °C - 401.31 °C (43.81%). ESI-MS, *m/z* Calcd. For [M+Na]$^+$ 932.8719. Found 932.8698.

4.5. Synthesis of synthesis of [(η^6-p-cymene)$RuCl_2$(μ-dppm)Fe(CO)I(η^5-C_5H_5)] (2)

0.1502 g (0.227 mmol) of [CpFe(CO)(κ^1-dppm)I] and 0.0722 g (0.118 mmol) of [Ru(η^6-p-$MeC_6H_4Pr^i$)Cl_2]$_2$ were dissolved in 10 mL of dried dichloromethane, and stirred for 30 min. The reaction was followed by TLC, which showed complete consumption of the starting material after 30 min. The solvent was removed *in vacuo* to isolate a brown solid and was washed with n-hexane (3 × 2 mL). After decanting the washings, the solid was dried under vacuum at room temperature. Air stable. 0.2151 g (0.223 mmol). Dark Brown solid (94.3%). Melting point 238 °C + dec. ^{1}H NMR ($CDCl_3$, 298.2 K): δ 8.10–7.05 (20H, m, C–*H*, dppm), 5.08 (2H, m, C^{3,5}-*H*, η^6-*p*-cymene), 4.97 (2H, m, C^{2,6}-*H*, η^6-*p*-cymene), 4.23 (5H, br s, η^5-C_5H_5), 2.86 (1H, m, $^2J_{HP}$ = 22.0 Hz, PCH_2P, H^B), 2.48 (1H, m, $^2J_{HP}$ = 18.3 Hz, PCH_2P, H^A), 1.72 (6H, d, $^2J_{HH}$ = 6.1 Hz, CH(CH_3)$_2$), 1.18 (3H, br s, CH_3), (C*H*$(CH_3)_2$ not visible). ^{13}C {^{1}H} NMR ($CDCl_3$, 298.2 K): δ 133.7 (br t, $^2J_{PC}$ = 6.5 Hz, dppm), 131.7–131.0 (br m, dppm), 129.4–128.8 (m, dppm), 126.7 (d, $^2J_{PC}$ = 8.8 Hz, dppm), 126.3 (br t, $^2J_{PC}$ = 10.6 Hz, dppm), 83.9 (d, $^2J_{PC}$ = 7.1 Hz, η^6-*p*-cymene) (other signals expected from coordinated ring not visible), 81.5 (s, η^5-C_5H_5), 29.2 (s, *C*H$(CH_3)_2$), 28.7 (m, PCH_2P), 21.4 (s, CH(*C*H_3)$_2$), 20.6 (s, *C*CH_3, η^6-*p*-cymene), (Fe*C*O not visible). ^{31}P {^{1}H} NMR ($CDCl_3$, 298.2 K): δ 63.2 (d, $^2J_{PP}$ = 44.1 Hz, Fe-PPh_2), 24.1 (d, $^2J_{PP}$ = 43.9 Hz, Ru-PPh_2). ^{1}H NMR (C_6D_6, 298.2 K): δ 7.81 (8H, br m, C–*H*, dppm), 6.87 (12H, br m, 13H, C–*H*, dppm), 5.14 (1H, br m, $^2J_{HP}$ = 6.81 Hz, H^A, PCH_2P), 4.97 (1H, br m, $^2J_{HP}$ = 5.3 Hz, H^B, PCH_2P), 4.88 (2H, br s, C^{3,5}-*H*, η^6-*p*-cymene), 4.76 (1H, br s, C^2–*H*, η^6-*p*-cymene), 4.41 (1H, br s, C^6–*H*, η^6-*p*-cymene), 4.00 (5H, s, η^5-C_5H_5), 2.67 (1H, sept, $^2J_{HH}$ = 5.34 Hz, C*H*$(CH_3)_2$), 1.85 (3H, s, CH_3), 0.92 (6H, br t, $^3J_{HH}$ = 7.5 Hz, CH(CH_3)$_2$). ^{31}P {^{1}H} NMR (C_6D_6, 298.2 K): δ 63.4 (d, $^2J_{PP}$ = 43.6 Hz, Fe-PPh_2), 25.1 (d, $^2J_{PP}$ = 43.8 Hz, Ru-PPh_2). FTIR: 3051 (w), 2959 (w), 1937 (br s, C≡O streching), 1483 (w), 1433 (m), 1375 (w), 1319 (w), 1263 (w), 1182 (br w), 1159 (w), 1096 (m), 1057 (w), 1028 (w), 999 (w), 839 (w), 822 (w), 797 (w), 731 (br, s), 692 (s), 623 (w), 608 (br w), 554 (br w). UV–Vis: (nm)/dichloromethane λ_{max} = 357.1. EIMS (70 eV) *m/z* 966.10 (<0.1%, M$^+$), 119.15 (100.0%, η^6-$C_6H_5Pr^i$ - H$^+$), 134.15 (30.64%, η^6-p-$MeC_6H_4Pr^i$), 350.0 (3.22%, Ru(η^6-p-MeC_6H_4-Pr^i)Cl_2), 384.20 (2.55%, $(Ph)_2P(CH_2)P(Ph)_2$), 400.20 (14.88%, O=$P(Ph)_2(CH_2)P(Ph)_2$), 678.10 (5.39%, CpFe(CO)(κ^1-dppm)I with H_2O adduct). ESI-MS, *m/z* Calcd. For [M+Na]$^+$ 988.9345. Found 988.9324.

4.6. Synthesis of [$RuCl_2$(η^6-C_6H_6)]$_2$(μ-dppm)] (3)

223 mg (0.367 mmol) of **4** was stirred with 88 mg (0.176 mmol) of [RuCl(μ-Cl)(η^6-C_6H_6)]$_2$ in DCM for 2.5h under reflux. The solvent was removed *in vacuo* to isolate a solid, which was then washed with diethyl ether (3 × 10 mL). After disposing of the washings; the solid was dried at room temperature. Air stable. 246 mg (0.278 mmol) of brown solid (70.2%). Melting point 180 °C + dec. ^{1}H NMR ($CDCl_3$, 298 K): δ 7.54 (4H, m, C^4–*H*, dppm), 7.33–7.25 (8H, m, C$^{3,5\ or\ 2,6}$–*H*, dppm), 7.18–7.10 (8H, m, C$^{2,6\ or\ 3,5}$–*H*, dppm), 5.31 (12H, s, η^6-C_6H_6), 4.70 (2H, t, $^2J_{PH}$ = 8.55 Hz, PCH_2P). ^{13}C {^{1}H} NMR ($CDCl_3$, 298 K): δ 133.7 (t, $^2J_{PC}$ = 4.1 Hz, C^{2,6}-dppm), 130.7 (s, C^4-dppm), 130.1 (d, $^1J_{PC}$ = 23.1 Hz, C^1-dppm), 127.7 (t, $^3J_{PC}$ = 5 Hz, C^{3,5}-dppm), 88.6 (s, η^6-C_6H_6), 25.7 (t, $^1J_{PC}$ = 9.9 Hz, PCH_2P). ^{31}P {^{1}H} NMR ($CDCl_3$, 298K): δ 22.6 (s, Ru-PPh_2). FTIR (cm^{-1}): 1482 (m), 1433 (vs), 1263 (m), 1096 (s), 1028 (vw), 1000 (w), 732 (s), 692 (s), 608 (m), 594 (w), 585 (m), 567 (w), 561 (w), 557 (vw), 554 (w), 548 (w), 542 (w), 539 (vw), 533 (w), 530 (m), 522 (w), 506 (m), 503 (m). UV–vis: (nm)/dichloromethane: λ 372.0. ESI-MS (THF), *m/z*: calcd for [$C_{37}H_{34}Ru_2P_2Cl_4$+Na]$^+$: 906.8844. Found: 906.8842.

4.7. Density functional theory calculations

DFT calculations were performed to model the complexes **1**, **2** and **3**. Guassian09 software package was used. For all the calculations, the level of theory used for all calculations is B3LYP with the basis set 6-31 + G(d,p) for H, C, O, P, I and Cl atoms; while for Ru and Fe atoms DGDZVP basis set was used. Geometry optimizations were calculated without any constrains. All the optimized geometries show not imaginary frequency. Energies were calculated on the optimized structures [29].

Associated content

The supporting information is available free of charge. Supporting Information is available with experimental details, NMR, IR and ESI-MS spectra, X-ray crystallographic details of **3** and Cartesian coordinates for the complexes studied by DFT methods.

Accession codes

CCDC 1936145 contain the supplementary crystallographic data for this paper. This data can be obtained free of charge via www.ccdc.cam.ac.uk/data_request/cif, or by emailing data_request@ccdc.cam.ac.uk, or by contacting The Cambridge Crystallographic Data Centre, 12 Union Road, Cambridge CB2 1EZ, UK; fax: +44 1223 336033.

Acknowledgements

We would like to thank the Maastricht Science Programme (MSP) and Maastricht University (Faculty of Science and Engineering) for financial support of this research. BB thanks numerous students who did some preliminary work in this area as part of a research project within the MSP. JB thanks the Austrian *Fonds zur Förderung der wissenschaftlichen Forschung* (FWF) via the project P-30955. Dr. Maria Schlangen-Ahl (TU Berlin) is thanked for recording HRMS of all complexes.

Appendix A. Supplementary data

Supplementary data to this article can be found online at https://doi.org/10.1016/j.jorganchem.2019.120934.

References

[1] B. Rosenberg, L. Vancamp, J.E. Trosko, V.H. Mansour, Nature 222 (5191) (1969) 385.
[2] (a) S. Manohar, N. Leung, J. Nephrol. 31 (1) (2018) 15;
(b) J. Hu, T.M. Wu, H.Z. Li, Z.P. Zuo, Y.L. Zhao, L. Yang, Bioorg. Med. Chem. Lett 27 (15) (2017) 3591;
(c) A. Wilmes, C. Bielow, C. Ranninger, P. Bellwon, L. Aschauer, A. Limonciel, H. Chassaigne, T. Kristl, S. Aiche, C.G. Huber, C. Guillou, P. Hewitt, M.O. Leonard, W. Dekant, F. Bois, P. Jennings, Toxicol. In Vitro: Int. J. Publ. Assoc. BIBRA 30 (1 Pt A) (2015) 117;
(d) S. Zhu, N. Pabla, C. Tang, L. He, Z. Dong, Arch. Toxicol. 89 (12) (2015) 2197;
(e) S. Dasari, P.B. Tchounwou, Eur. J. Pharmacol. 740 (2014) 364;
(f) N.D. Eljack, H.Y. Ma, J. Drucker, C. Shen, T.W. Hambley, E.J. New, T. Friedrich, R.J. Clarke, Metallomics 6 (11) (2014) 2126;
(g) L.A. Peres, A.D. da Cunha Jr., Jornal brasileiro de nefrologia : 'orgao oficial de Sociedades Brasileira e Latino-Americana de Nefrologia 35 (4) (2013) 332;
(h) J.T. Hartmann, H.P. Lipp, Expert Opin. Pharmacother. 4 (6) (2003) 889.
[3] (a) D.J. Crona, A. Faso, T.F. Nishijima, K.A. McGraw, M.D. Galsky, M.I.A. Milowsky, The Oncologist 22 (5) (2017) 609;
(b) S. Spreckelmeyer, N. Estrada-Ortiz, G.G.H. Prins, M. van der Zee, B. Gammelgaard, S. Sturup, I.A.M. de Graaf, G.M.M. Groothuis, A. Casini, Metallomics 9 (12) (2017) 1786;
(c) C.M. Driessen, M.J. Uijen, W.T. van der Graaf, C.C. van Opstal, J.H. Kaanders, T. Nijenhuis, C.M. van Herpen, Head Neck 38 (Suppl 1) (2016) E1575–E1581;
(d) J. Zhao, Pharmacol. Ther. 160 (2016) 145;
(e) J.A. Ferreira, A. Peixoto, M. Neves, C. Gaiteiro, C.A. Reis, Y.G. Assaraf, L.L. Santos, Drug Resist. Updates 24 (2016) 34;
(f) R.S. Goldstein, G.H. Mayor, Life Sci. 32 (7) (1983) 685.
[4] See as examples: (a) M. Miyamoto, M. Takano, M. Kuwahara, H. Soyama, K. Kato, H. Matuura, T. Sakamoto, K. Takasaki, T. Aoyama, T. Yoshikawa, K. Furuya, Cancer Chemother. Pharmacol. 81 (1) (2018) 111;
(b) Y. Wang, L. Wang, G. Chen, S. Gong, Macromol. Biosci. 17 (5) (2017) 1600292;
(c) L.-Y. Wang, H. Xie, H. Zhou, W.-X. Yao, X. Zhao, Y. Wang, Saudi Med. J. 38 (1) (2017) 18;
(d) T. Ozdian, D. Holub, Z. Maceckova, L. Varanasi, G. Rylova, J. Rehulka, J. Vaclavkova, H. Slavik, P. Moudry, P. Znojek, J. Stankova, J.B. de Sanctis, M. Hajduch, P. Dzubak, J. Proteomics 162 (2017) 73;
(e) J. Zheng, X. Feng, W. Hu, J. Wang, Y. Li, Medicine (Baltim.) 96 (13) (2017) e6487;
(f) G.Y. Ho, N. Woodward, J.I. Coward, Crit. Rev. Oncol.-Hematol. 102 (2016) 37;
(g) W. Wei, Z. Liu, X. Chen, F. Bi, Int. J. Clin. Pharm. Ther. 52 (8) (2014) 702;
(h) L.M. Pasetto, M.R. D'Andrea, A.A. Brandes, E. Rossi, S. Monfardini, Crit. Rev. Oncol. Hematol. 60 (1) (2006) 59;
(i) A. Ghezzi, M. Aceto, C. Cassino, E. Gabano, D. Osella, J. Inorg. Biochem. 98 (1) (2004) 73;
(j) C.-H. Choi, Y.-J. Cha, C.-S. An, K.-J. Kim, K.-C. Kim, S.-P. Moon, Z.H. Lee, Y.-D. Min, Cancer Cell Int. 4 (1) (2004) 6.
[5] (a) P. Ringhieri, G. Morelli, A. Accardo, Crit. Rev. Ther. Drug Carrier Syst. 34 (2) (2017) 149;
(b) I.E. Leon, J.F. Cadavid-Vargas, A.L. Di Virgilio, S.B. Etcheverry, Curr. Med. Chem. 24 (2) (2017) 112;
(c) J.-X. Liang, H.-J. Zhong, G. Yang, K. Vellaisamy, D.-L. Ma, C.-H. Leung, J. Inorg. Biochem. 177 (2017) 276;
(d) T. Lazarević, A. Rilak, Ž.D. Bugarčić, Eur. J. Med. Chem. 142 (2017) 8;
(e) K.M. Deo, B.J. Pages, D.L. Ang, C.P. Gordon, J.R. Aldrich-Wright, Int. J. Mol. Sci. 17 (11) (2016) 1818;
(f) I. Potočňák, P. Vranec, V. Farkasová, D. Sabolová, M. Vataščinová, J. Kudláčová, I.D. Radojević, L.R. Čomić, B.S. Markovic, V. Volarevic, N. Arsenijevic, S.R. Trifunović, J. Inorg. Biochem. 154 (2016) 67;
(g) C.S. Allardyce, P.J. Dyson, Dalton Trans. 45 (8) (2016) 3201;
(h) C.R. Munteanu, K. Suntharalingam, Dalton Trans. 44 (31) (2015) 13796;
(i) L. Massai, J. Fernandez-Gallardo, A. Guerri, A. Arcangeli, S. Pillozzi, M. Contel, L. Messori, Dalton Trans. 44 (24) (2015) 11067;
(j) D. Denoyer, S. Masaldan, S. La Fontaine, M.A. Cater, Metallomics 7 (11) (2015) 1459;
(k) A. Winter, M. Gottschaldt, G.R. Newkome, U.S. Schubert, Curr. Top. Med. Chem. 12 (3) (2012) 158.
[6] (a) W. Su, Y. Li, P. Li, Mini Rev. Med. Chem. 18 (2) (2018) 184;
(b) L. Zeng, P. Gupta, Y. Chen, E. Wang, L. Ji, H. Chao, Z.-S. Chen, Chem. Soc. Rev. 46 (19) (2017) 5771;
(c) L. Biancalana, G. Pampaloni, F. Marchetti, Chimia 71 (9) (2017) 573;
(d) A. Notaro, G. Gasser, Chem. Soc. Rev. 46 (23) (2017) 7317;
(e) M. Abid, F. Shamsi, A. Azam, Mini Rev. Med. Chem. 16 (10) (2016) 772;
(f) E.S. Antonarakis, A. Emadi, Cancer Chemother. Pharmacol. 66 (1) (2010) 1;
(g) I. Kostova, Curr. Med. Chem. 13 (9) (2006) 1085.
[7] (a) G.E. Davey, Z. Adhireksan, Z. Ma, T. Riedel, D. Sharma, S. Padavattan, D. Rhodes, A. Ludwig, S. Sandin, B.S. Murray, P.J. Dyson, C.A. Davey, Nat. Commun. 8 (2017) 1575;
(b) B. Thulasiram, C.S. devi, Y.P. Kumar, R.R. Aerva, S. Satyanarayana, P. Nagababu, J. Fluoresc. 27 (2) (2017) 587;
(c) C.S. Devi, B. Thulasiram, S. Satyanarayana, P. Nagababu, J. Fluoresc. 27 (6) (2017) 2119;
(d) G. Sava, S. Pacor, F. Bregant, V. Ceschia, Anticancer Res. 11 (3) (1991) 1103;
(e) L. Zeng, P. Gupta, Y. Chen, E. Wang, L. Ji, H. Chao, Z.-S. Chen, Chem. Soc. Rev. 46 (2017) 5771.
[8] See as an early example: F. Kratz, L. Messori J. Inorg. Biochem. 49 (1993) 79.
[9] (a) M. Pal, U. Nandi, D. Mukherjee, Eur. J. Med. Chem. 150 (2018) 419;
(b) J.B. Vincent, S. Love, Biochim. Biophys. Acta Gen. Subj. 1820 (3) (2012) 362;
(c) C.A. Smith, A.J. Sutherland-Smith, F. Kratz, E.N. Baker, B.H. Keppler, B.K. Keppler, J. Biol. Inorg. Chem. 1 (5) (1996) 424.
[10] (a) E. Allessio, Eur. J. Inorg. Chem. (2017) 1549;
(b) K. Śpiewak, M. Brindell, J. Biol. Inorg. Chem. 20 (4) (2015) 695;
(c) O. Mazuryk, K. Kurpiewska, K. Lewiński, G. Stochel, M. Brindell, J. Inorg. Biochem. 116 (2012) 11.
[11] (a) S. Chatterjee, S. Kundu, A. Bhattacharyya, C.G. Hartinger, P.J. Dyson, J. Biol. Inorg. Chem. 13 (7) (2008) 1149;
(b) C. Scolaro, A.B. Chaplin, C.G. Hartinger, A. Bergamo, M. Cocchietto, B.K. Keppler, G. Sava, P.J. Dyson, Dalton Trans. 43 (2007) 5065;
(c) C. Scolaro, T.J. Geldbach, S. Rochat, A. Dorcier, C. Gossens, A. Bergamo, M. Cocchietto, I. Tavernelli, G. Sava, U. Rothlisberger, Organometallics 25 (3) (2006) 756;
(d) C. Deacon-Price, D. Romano, T. Riedel, P.J. Dyson, B. Blom, Inorg. Chim. Acta 484 (2019) 513;
(e) R.F. Brissos, P. Clavero, A. Gallen, A. Grabulosa, L.A. Barrios, A.B. Caballero, L. Korrodi-Gregorio, R. Perez-Tomas, G. Muller, V. Soto-Cerrato, P. Gamez, Inorg. Chem. 57 (23) (2018) 14786;
(f) A. Ratanaphan, T. Nhukeaw, K. Hongthong, P.J. Dyson, Anti Cancer Agents Med. Chem. 17 (2) (2017) 212.
[12] (a) R.H. Berndsen, A. Weiss, U.K. Abdul, T.J. Wong, P. Meraldi, A.W. Griffioen, P.J. Dyson, P. Nowak-Sliwinska, Sci. Rep. 7 (2017) 43005;
(b) A. Weiss, X. Ding, J.R. van Beijnum, I. Wong, T.J. Wong, R.H. Berndsen, O. Dormond, M. Dallinga, L. Shen, R.O. Schlingemann, R. Pili, C.M. Ho, P.J. Dyson, H. van den Bergh, A.W. Griffioen, P. Nowak-Sliwinska, Angiogenesis 18 (3) (2015) 233.
[13] (a) E. Alessio, L. Messori, Molecules 24 (10) (2019) 1995;
(b) B.G. Dwyer, E. Johnson, E. Cazares, K.L. McFarlane Holman, S.R. Kirk, J. Inorg. Biochem. 182 (2018) 177;
(c) G.K. Gransbury, P. Kappen, C.J. Glover, J.N. Hughes, A. Levina, P.A. Lay, I.F. Musgrave, H.H. Harris, Metallomics 8 (8) (2016) 762.
[14] (a) R. Pettinari, A. Petrini, F. Marchetti, C. Pettinari, T. Riedel, B. Therrien, P.J. Dyson, Eur. J. Inorg. Chem. (2017) 1800;
(b) C.G. Hartinger, M.A. Jakupec, S. Zorbas-Seifried, M. Groessl, A. Egger, W. Berger, H. Zorbas, P.J. Dyson, B.K. Keppler, Chem. Biodivers. 5 (10) (2008) 2140;
(c) C.G. Hartinger, S. Zorbas-Seifried, M.A. Jakupec, B. Kynast, H. Zorbas, B.K. Keppler, J. Inorg. Biochem. 100 (5–6) (2006) 891;
(d) F. Marchetti, R. Pettinari, C. Di Nicola, C. Pettinari, J. Palmucci, R. Scopelliti, T. Riedel, B. Therrien, A. Galindo, P.J. Dyson, Dalton Trans. 47 (3) (2018) 868;
(e) C.P. Popolin, J.P.B. Reis, A.B. Becceneri, A.E. Graminha, M.A.P. Almeida, R.S. Corrêa, L.A. Colina-Vegas, J. Ellena, A.A. Batista, M.R. Cominetti, PLoS One 12 (9) (2017), e0183275;
(f) S.M. Page, S.R. Boss, P.D. Barker, Future Med. Chem. 1 (3) (2009) 541.
[15] (a) R.A. Khan, A. Asim, R. Kakkar, D. Gupta, V. Bagchi, F. Arjmand, S. Tabassum,

Organometallics 32 (9) (2013) 2546;
(b) J. Schulz, A.K. Renfrew, I. Císařová, P.J. Dyson, P. Štěpnička, Appl. Organomet. Chem. 24 (5) (2010) 392;
(c) M. Velayudham, S. Rajagopal, Polyhedron 28 (14) (2009) 3043;
(d) C. Cornelissen, G. Erker, G. Kehr, R. Fröhlich, Organometallics 24 (2) (2005) 214.

[16] (a) A. Pilon, P. Gírio, G. Nogueira, F. Avecilla, H. Adams, J. Lorenzo, M.H. Garcia, A. Valente, J. Organomet. Chem. 852 (2017) 34;
(b) T.S. Morais, A. Valente, A.I. Tomaz, F. Marques, M.H. Garcia, Future Med. Chem. 8 (5) (2016) 527;
(c) H.T. Poh, P.C. Ho, W.Y. Fan, RSC Adv. 6 (23) (2016) 18814;
(d) P.R. Florindo, D.M. Pereira, P.M. Borralho, C.M.P. Rodrigues, M.F.M. Piedade, A.C. Fernandes, J. Med. Chem. 58 (10) (2015) 4339;
(e) A.C. Gonçalves, T.S. Morais, M.P. Robalo, F. Marques, F. Avecilla, C.P. Matos, I. Santos, A.I. Tomaz, M.H. Garcia, J. Inorg. Biochem. 129 (2013) 1.

[17] A search for bimetallic Fe,Ru complexes bridged with $R_2P(CH_2)_nPR_2$ (n = 1, 2, 3) yielded surpisingly few results. See: (a) N. Nawar, A.K. Smith, J. Organomet. Chem. 493 (1) (1995) 239;
(b) P.A. Dolby, M.M. Harding, N. Newar, A.K. Smith, J. Chem. Soc., Dalton Trans. (1992) 2939;
(c) T. Venäläinen, E. Iiskola, J. Pursiainen, T.A. Pakkanen, T.T. Pakkanen, J. Mol. Catal. 34 (3) (1986) 293;
(d) A.W. Coleman, D.F. Jones, P.H. Dixneuf, C. Brisson, J.J. Bonnet, G. Lavigne, Inorg. Chem. 23 (7) (1984) 952.

[18] (a) R.J. Haines, A.L. du Preez, Inorg. Chem. 11 (1972) 330;
(b) D. Serra, M.C. Correia, L. McElwee-White, *Organometallics* 30 (21) (2011) 5568;
(c) D. Serra, K.A. Abboud, C.R. Hilliard, L. McElwee-White, Organometallics 26 (13) (2007) 3085.

[19] High-spin low-spin equilibria are rather common for Fe(II) complexes (t_{2g}^6 vs $t_{2g}^4e_g^2$ for Octahedral Configured Species) which leads to line broadening which can be reduced at lower temperatures. As an example of this see the behavior of the complex $[Fe(depe)_2Cl_2]$ (Depe = 1,1-bis(diethylphosphino)ethane B.Blom, PhD dissertation, University of Bonn, 2011.

[20] (a) R.A. Zelonka, M.C. Baird, Can. J. Chem. 50 (18) (1972) 3063;
(b) R.A. Zelonka, M.C. Baird, J. Organomet. Chem. 44 (2) (1972) 383.

[21] (a) A.W. Coleman, H. Zhang, S.G. Bott, J.L. Atwood, P.H. Dixneuf, J. Coord. Chem. 16 (1) (1987) 9;
(b) F. Estevan, P. Lahuerta, J. Latorre, A. Sanchez, C. Sieiro, Polyhedron 6 (3) (1987) 473;
(c) A.W. Coleman, D.F. Jones, P.H. Dixneuf, C. Brisson, J.J. Bonnet, G. Lavigne, Inorg. Chem. 23 (7) (1984) 952.

[22] (a) A.B. Chaplin, C. Fellay, G. Laurenczy, P.J. Dyson, Organometallics 26 (3) (2007) 586;
(b) D.K. Gupta, A.N. Sahay, D.S. Pandey, N.K. Jha, P. Sharma, G. Espinosa, A. Cabrera, M.C. Puerta, P. Valerga, J. Organomet. Chem. 568 (1) (1998) 13;
(c) A.W. Coleman, H. Zhang, S.G. Bott, J.L. Atwood, P.H. Dixneuf, J. Coord. Chem. 16 (1) (1987) 9.

[23] Interestingly, in our Hands, the reactions of **4** and **4-cym** with Cisplatin in an attempt to prepare the Heterobimetallic Ru,Pt Complexes of the Type $[(\eta^6\text{-Arene})Cl_2Ru(\mu\text{-dppm})PtCl_2(NH_3)]$ (Arene = C_6H_6 or *P*-Cymene) by NH_3 substitution at the Pt(II) centre also afforded a Mixture of **3** and $[PtCl_2(\kappa^2\text{-Dppm})]$ or **3-cym** and $[PtCl_2(\kappa^2\text{-Dppm})]$ respectively, confirmed on the basis of ^{31}P and ^1H NMR Spectroscopy and comparison to authentic samples.

[24] T. Mosmann, J. Immunol. Methods 65 (1983) 55.

[25] SAINT+ Version 6.45, Bruker Analytical X-Ray Systems. *Inc.*, Madison, Wisconsin, USA, 2003.

[26] G.M. Sheldrick, SADABS v. 2.10, Bruker AXS Inc., Madison, Wisconsin, USA, 2003.

[27] R.H. Blessing, Acta Crystallogr. A 51 (1) (1995) 33.

[28] (a) G.M. Sheldrick, Acta Crystallogr. C: Struct. Chem. 71 (1) (2015) 3;
(b) G.M. Sheldrick, Acta Crystallogr. A: Found. Crystallogr. 64 (1) (2008) 112.

[29] M.J. Frisch, G.W. Trucks, H.B. Schlegel, G.E. Scuseria, M.A. Robb, J.R. Cheeseman, G. Scalmani, V. Barone, B. Mennucci, G.A. Petersson, H. Nakatsuji, M. Caricato, X. Li, H.P. Hratchian, A.F. Izmaylov, J. Bloino, G. Zheng, J.L. Sonnenberg, M. Hada, M. Ehara, K. Toyota, R. Fukuda, J. Hasegawa, M. Ishida, T. Nakajima, Y. Honda, O. Kitao, H. Nakai, T. Vreven, J.A. Montgomery Jr., J.E. Peralta, F. Ogliaro, M. Bearpark, J.J. Heyd, E. Brothers, K.N. Kudin, V.N. Staroverov, R. Kobayashi, J. Normand, K. Raghavachari, A. Rendell, J.C. Burant, S.S. Iyengar, J. Tomasi, M. Cossi, N. Rega, J.M. Millam, M. Klene, J.E. Knox, J.B. Cross, V. Bakken, C. Adamo, J. Jaramillo, R. Gomperts, R.E. Stratmann, O. Yazyev, A.J. Austin, R. Cammi, C.J. Pomelli, W. Ochterski, R.L. Martin, K. Morokuma, V.G. Zakrzewski, G.A. Voth, P. Salvador, J.J. Dannenberg, S. Dapprich, A.D. Daniels, O. Farkas, J.B. Foresman, J.V. Ortiz, J. Cioslowski, Gaussian 09, Revision D.01, Gaussian, Inc., Wallingford, CT, 2009.